Available online at www.sciencedirect.com
ScienceDirect
Journal of Sound and Vibration 297 (2006) 649–663
JOURNAL OF SOUND AND VIBRATION
www.elsevier.com/locate/jsvi

Experimental simulation of the sharpening process of a disc blade and analysis of its dynamic response

C. Carmignani, P. Forte*, E. Rustighi[1]

University of Pisa, Department of Mechanical, Nuclear and Production Engineering, via Diotisalvi 2, 56126 Pisa, Italy

Received 7 October 2004; received in revised form 10 April 2006; accepted 12 April 2006
Available online 21 June 2006

Abstract

The vibrations arising in the sharpening of large disc blades used in paper roll cutting machines are a crucial problem for paper manufacturing quality. In this work the results of an experimental investigation carried out on a reduced scale versatile test rig are presented and discussed. A series of tests were carried out varying the characteristic parameters of the process such as the grinding contact force, the contact friction, the grinding wheel and blade relative positions, and the sharpening time length. The Fourier transform was applied to the disc displacement signals and analyses of the waterfall plots obtained for the different cases show the influence of the operation and design parameters on the system dynamic behaviour.

1. Introduction

Vibrations arising during the sharpening process of disc blades are a crucial problem in paper manufacturing. In particular, since paper rolls are cut by disc blades, defects in the blade edge caused by vibrations in sharpening, though small, can cause remarkable quality and productivity losses. Common practice has shown that in some cases the disc edge exhibits a periodic thickness irregularity caused by such vibrations. In the technical literature no specific work is reported but similar problems such as those related to grinding [1], saw blades, turbine rotors, computer magnetic recording discs [2,3] and brake discs [4–6] are dealt with.

The problems mainly concern the response of a rotating disc to an external transverse force. It is well established [7–12] that a rotating disc, with respect to an inertial frame, displays a response that can be viewed as the superposition of a forward travelling wave motion and a backward travelling wave motion. With increasing disc rotational speed the frequency associated with the backward travelling wave approaches zero and a divergence instability arises, led by a transverse load applied to the rotating disc. The disc rotational speed at which this happens is identified as a critical speed [13].

*Corresponding author.
E-mail addresses: carmi@ing.unipi.it (C. Carmignani), p.forte@ing.unipi.it (P. Forte), er@isvr.soton.ac.uk (E. Rustighi).
[1]Present Address: University of Southampton, Institute of Sound and Vibration Research, Southampton SO17 1BJ, UK.

0022-460X/$ - see front matter
doi:10.1016/j.jsv.2006.04.018

Another type of instability occurs on account of the coalescence of two vibratory modes. This phenomenon, called lock-in instability, may be due to the coupling of natural modes of the contacting parts. In the case of a pin-on disc system this coupling depends on the relation between the tangential force that excites bending vibrations of the pin and the transverse force that excites the disc. That relation may be due to pin inclination or to friction [6,14].

Moreover interface friction couples longitudinal and transversal degrees of freedom making the system potentially unstable. The motion may become intermittent with stick and slip phases [15]. Unfortunately friction vibrations are quite often unpredictable because the dependency of friction on velocity varies randomly with contamination, surface finish, misalignment of sliding surfaces and other factors.

In previous work, Carmignani et al. [16] simulated the sharpening process of a disc blade by means of the explicit finite element code LS-DYNA®. Some phenomenological aspects were shown highlighting the most important parameters affecting them such as stiffness, contact force and rotational speed. The results of an experimental investigation carried out on a commercial paper cutting machine with fixed operating parameters were also presented and discussed.

This paper reports the experimental work carried out on a versatile test rig designed and set up to study the vibrations arising in the sharpening process of disc blades and the influence of different operation and design parameters. Preliminary analytical work supported the analysis of the experimental results in the identification of the vibratory modes, including modal analyses of the finite element models of the test rig components.

2. The test rig

The test rig (Figs. 1 and 2) was designed to reproduce the sharpening process allowing the parameters of the process to be easily varied.

The sharpening process in the machine is achieved by means of the translation of a face grinding wheel that is pushed on the disc by a pre-loaded spring. The disc is made of steel and has a 380 mm outer diameter and a 40 mm inner hole. Its standard thickness is 3 mm but discs with different thickness can be tested. The disc is fastened to a rotating shaft by an annular clamp with outer radius of 45 mm. Clamping discs with different

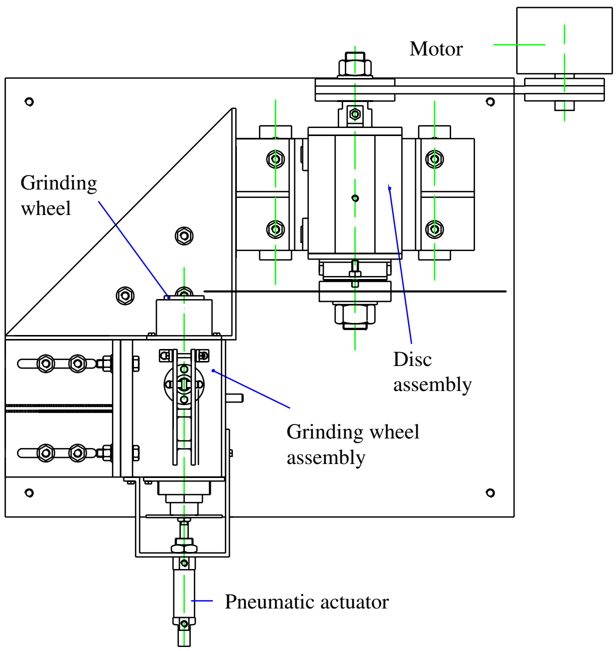

Fig. 1. Schematic top view of the test rig.

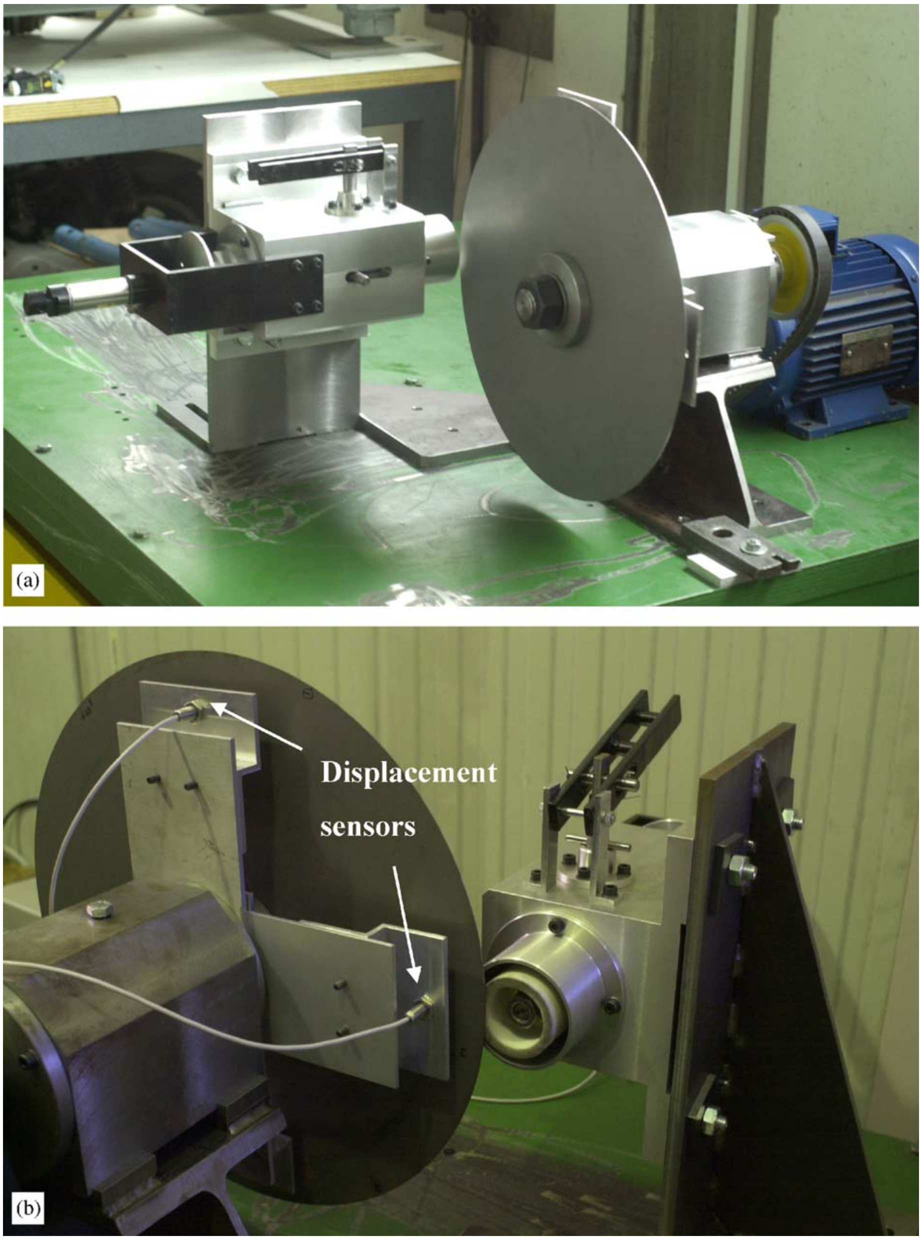

Fig. 2. Photo of the test rig: (a) front view and (b) rear view.

diameters can be used in order to change the radius of the inner constraint on the disc and consequently change its natural frequencies. The face grinding wheel is cylindrical with a 50 mm outer diameter.

The disc shaft is quite stiff so as not to affect the vibrational behaviour of the flexible disc. The rotational motion is transmitted to the shaft by an asynchronous three-phase motor through a belt drive. The rotational speed can be varied continuously by means of an inverter controlled by a PC up to 1500 rev/min which is a common operating speed for sharpening commercial machines.

The shaft rotational velocity can be inferred by processing the signal of a displacement non-contacting transducer (Proximitor®) triggered by grooves on the shaft. Similar sensors, placed on plate supports fitted on the bearing block, measure the disc out-of-plane displacements. Each plate support can be placed independently from the others at any angular position. Moreover the sensors can be moved radially.

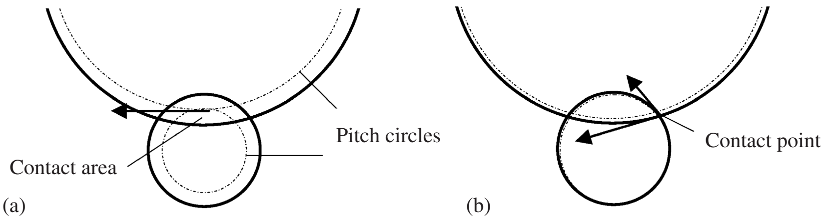

Fig. 3. Schematic of the disc and grinding wheel contact conditions and velocity vectors in (a) parallel configuration and (b) tilted configuration.

The grinding wheel shaft is fitted inside an axially translating sleeve by means of two rolling bearings so that it can freely move axially and rotate at the same time. The rotating disc drags the grinding wheel due to friction. The rotation of the abrasive wheel shaft can eventually be blocked.

The translating system is pushed against the disc by a spring whose pre-load can be continuously varied from almost 0–200 N by means of a thread sleeve. The translating system has a 1.3 kg mass and the pushing spring has a 16.6 N/mm stiffness coefficient. The resulting natural translating frequency is about 113 rad/s (18 Hz), corresponding to the natural frequency of the commercial paper cutting machine. However such a frequency can be easily modified by changing the pushing spring. A proximity probe measures the axial vibration of the grinding wheel. The translation of the grinding wheel is driven by unlocking the translating sleeve either manually or by a pneumatic actuator driven by a PC-controlled solenoid valve so that different sharpening sequences can be set.

In the reference configuration the disc and the grinding wheel rotational axes are parallel and the contact occurs on an area by the disc edge (Fig. 3(a)), in rolling sliding friction conditions. The rotational axis of the grinding wheel can be tilted by 2° on a plane tangent to the disc edge. Thus the contact occurs on a point of the disc edge (Fig. 3(b)). The pitch circles of the two bodies, projected on the same plane, are no longer tangent but cross each other in the contact point where the velocity vectors are no longer parallel. Therefore the grinding wheel rotational frequency will be likely lower than in the reference case and there will be also a relative velocity component and consequent sliding friction. Actually in the commercial paper cutting machine taken as a reference, the disc blade has a tapered edge and the grinding wheel shaft is inclined both radially and tangentially with respect to the disc blade. The grinding wheel radial inclination corresponds to the angle of the conical edge surface. For the sake of manufacturing simplicity and to focus the investigation on the coupling between the disc nodal diameter modes and the grinding wheel modes that seemed the likely cause of the blade sharpening defects, the test rig disc was made flat and only the tangential inclination was reproduced.

The equipment is driven and sensor data are acquired by a PC provided with the National Instruments DAQ board PC-M10-16E-4 through specific programs developed in the LabVIEW™ environment. The DAQ system includes an antialiasing filter.

3. Experimental investigation

In order to evaluate the effect of each parameter on the onset of self-excited vibrations during the sharpening process, a reference sharpening test whose conditions are summarised in Table 1 was performed. The sharpening process was intermittent, namely a 1 s sharpening was followed by a 1 s break and again by a 1 s sharpening. The test was repeated at different rotational speeds of the disc: the speed was increased from 100 rev/min (1.6 Hz) up to 1500 rev/min (25 Hz) in 100 rev/min steps.

The other tests were carried out changing only one parameter at a time and the results were compared with the reference test results. The variations of the test conditions are listed in Table 1. They are mainly focused on the contact conditions between the abrasive wheel and the disc, including a reduction of the spring pre-load, water lubrication of the contact surface to reduce friction, locking of the grinding wheel idle rotation to increase the sliding velocity, tilting the axis of the grinding wheel by 2° to reduce the contact area, and different continuous sharpening intervals.

Table 1
Reference and variations of test conditions

Test conditions	Reference	Variation
Spring pre-load	50 N	25 N
Lubrication	No	Water
Grinding wheel rotation	Idle	Locked
Grinding wheel tilting angle	0°	2°
Sharpening sequence	1 s/1 s break/1 s	1 s; 5 s
Disc thickness	3 mm	1 mm

Some tests were carried out also on a 1 mm thick disc. Such a disc proved to be too compliant and, in order to keep the vibration amplitudes small, a very low pre-load was applied to the pushing spring and the maximum rotation speed was limited to 1100 rev/min.

3.1. Impact modal testing

The modal characteristics of the disc and of the grinding wheel support were preliminarily found by impact tests.

A modal hammer and an accelerometer were used. The hammer was equipped with a plastic tip, which can excite the structure up to 500 Hz. The cut-off frequency of the antialiasing filter was also 500 Hz. Acceleration data acquisition was triggered by the force signal of the impact hammer.

The force signal was windowed with a rectangular window and the acceleration signal with an exponential window. The transfer function of the system was estimated from the input (force) and output (acceleration) signals by the MATLAB® *tfe* function. Such a function finds a transfer function estimate Txy, as the quotient of the cross spectrum of the input signal vector **x** and of the output signal vector **y**, P_{xy}, and the power spectrum of **x**, P_{xx}:

$$T_{xy}(f) = \frac{P_{xy}(f)}{P_{xx}(f)}, \tag{1}$$

where f is the frequency. Such an estimate is useful to reduce the negative effects of a noisy output signal.

The disc was hit on its edge, perpendicularly to its plane. The accelerometer was placed diametrally opposite. The recorded peaks of T_{xy} (shown in Fig. 4) and natural frequencies (listed in Table 2) were correlated to the natural modes identified by the number of nodal diameters and nodal circles (*n,m*). In particular a very pronounced peak was detected at 263 Hz associated with the (3,0) mode. A preliminary FEM modal analysis eased the correlation of natural frequencies and modes (Fig. 5).

As far as the abrasive wheel support is concerned, since the natural frequency of the wheel shaft in the axial direction was set (it was designed for 18 Hz), the modal analysis regarded the natural frequencies of the structure in the direction perpendicular to the axis. The support was hit with the modal hammer near the joint point of the abrasive wheel in the vertical and horizontal directions. The accelerometer was placed on the opposite side of the structure.

Figs. 6(a) and (b) show the estimation of the transfer function of the structure in the vertical and horizontal direction, respectively. The coherence of the signals was greater than 0.99 in all the frequency range of interest proving the validity of the results. Table 3 lists all the modal frequencies of the support. Both the vertical and horizontal impact tests showed modes in the intervals around the frequencies of 50, 70 and 86 Hz, imputed to the translating sleeve; the measured natural frequencies are different in the two impact directions because the sleeve is not axial symmetric but the vertical and horizontal axial planes are planes of symmetry. The higher frequencies are associated to the support stem modes. In the vertical transfer function estimate the stem bending mode at 250 Hz was the most excited. During the horizontal test the stem torsional mode at 130 Hz was the most excited; since the torsion occurs around a vertical axis such a mode was not excited in the vertical impact test.

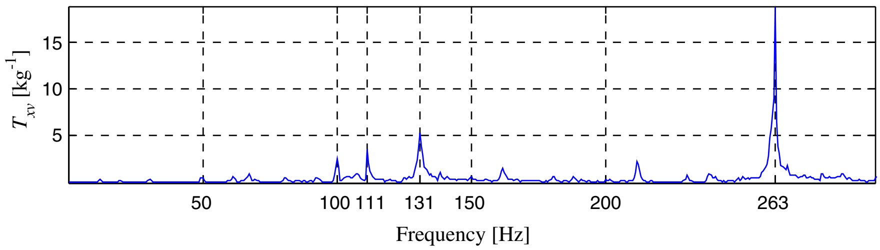

Fig. 4. Impact test of the disc: transfer function estimation (T_{xy}).

Table 2
Experimental modal testing results of the rig disc

Mode (n,m)	(0,0)	(1,0)	(2,0)	(3,0)
Nat. freq (Hz)	111	100	131	263

(n,m) are the number of nodal diameters and circles.

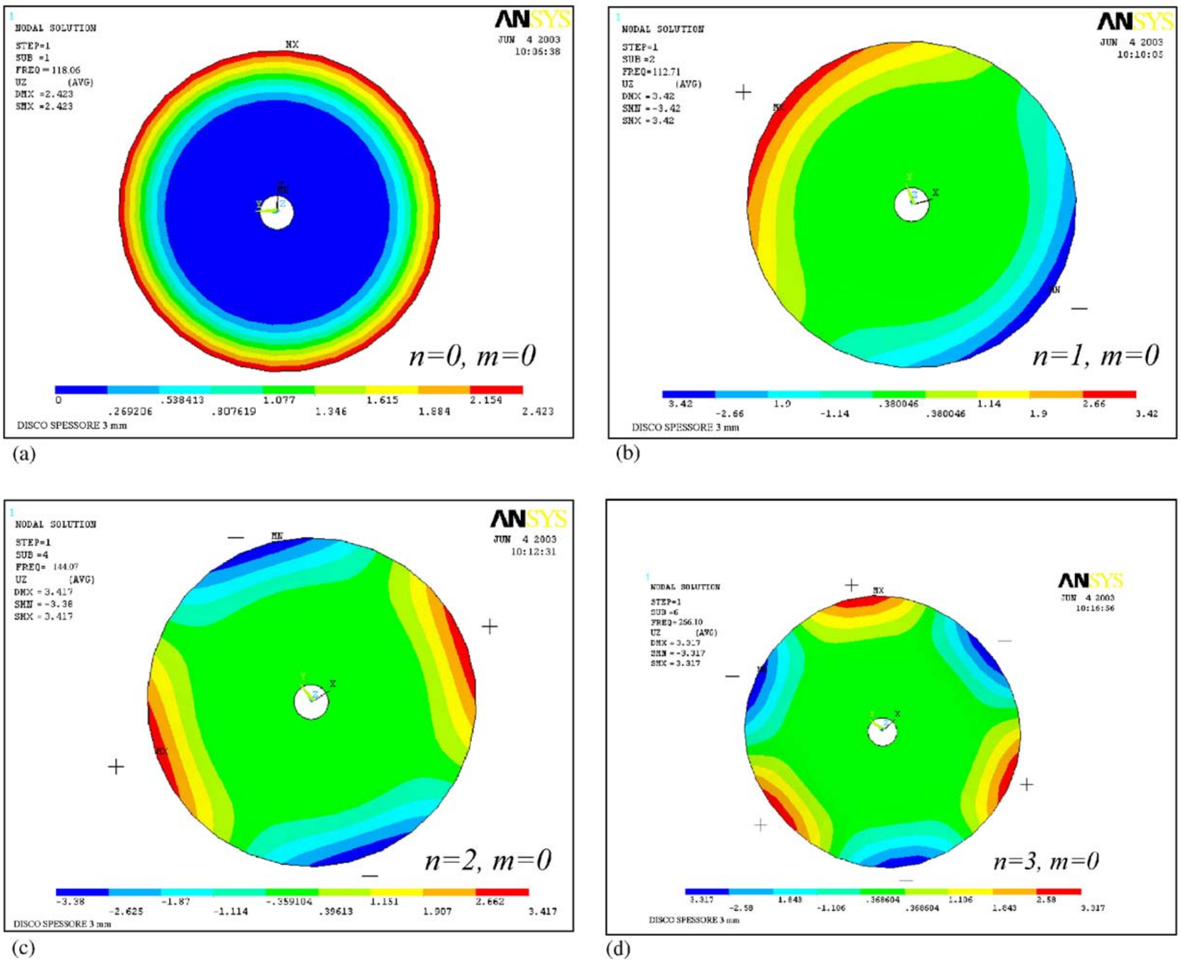

Fig. 5. Disc first modes obtained by FE modal analysis, n number of nodal diameters, m number of nodal circles.

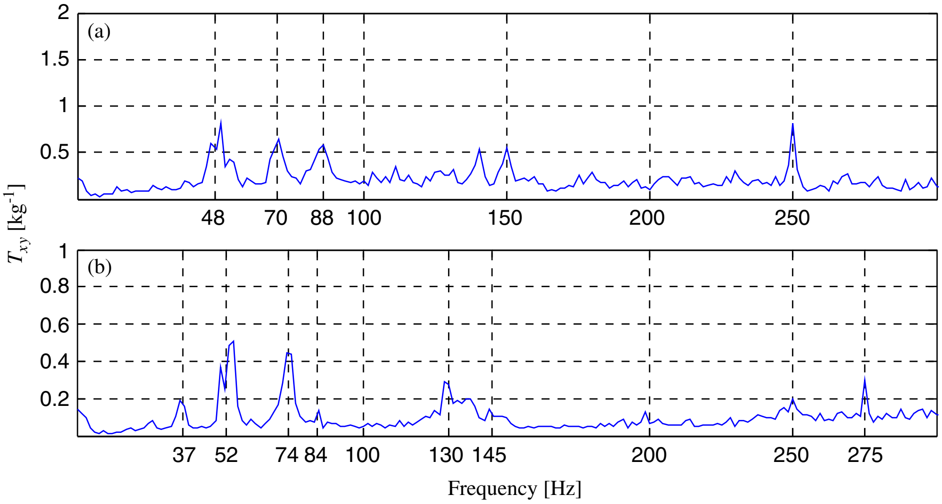

Fig. 6. Impact test of the grinding wheel support: (a) vertical and (b) horizontal transfer function estimations (T_{xy}).

Table 3
Experimental modal testing results of the rig support of the abrasive wheel

		Sleeve modes	Support stem modes
Natural frequencies (Hz)	Vertical	**48**; **70**; **86**	140; 150; **250**
	Horizontal	37; **52**; **74**; 84	**130**; 145; 200; 250; **275**

Most significant frequencies in bold.

3.2. Signal analysis

When conventional techniques are applied to a rotating disc, the Fourier transforms of the signals lose the directivity information of the forward and backward travelling waves, since the measured signals are treated as real quantities. In fact the spectra of real signals are symmetrical with respect to the origin of the frequency axis and the peak tracks of forward and backward travelling waves are present with their conjugates. Thus the two-sided Fourier transform of a real signal has four peaks for each mode as shown in Fig. 7.

It is possible to cancel mode peaks or alternatively their conjugates depending on the phase angle α between the disc displacement sensors by applying the two-sided integral Fourier transform to the complex signal $p = w_1 + \mathrm{i}w_2$ where w_1 and w_2 are the displacement signals of two sensors. This approach is at the basis of the directional frequency response function technique [12], which proved to be very effective in modal analysis to identify and separate forward and backward travelling waves for each mode of interest.

Briefly, let us consider the out-of-plane displacements w_1 and w_2 due to a single mode (i.e. due to two travelling waves) given by

$$w_1 = \cos(-\Omega t), \tag{2}$$

$$w_2 = \cos(n\alpha - \Omega t), \tag{3}$$

where Ω is the rotational velocity. The integral Fourier transform of the signal $p = w_1 + \mathrm{i}w_2$ is given by

$$\begin{aligned} F[\cos(-\Omega t) + i\cos(n\alpha - \Omega t)] = \sqrt{\frac{\pi}{2}}\big\{\delta(\omega - \Omega)[1 - \sin(n\alpha)] \\ + \delta(\omega + \Omega)[1 + \sin(n\alpha)] + i\cos(n\alpha)[\delta(\omega - \Omega) + \delta(\omega + \Omega)]\big\} \end{aligned} \tag{4}$$

where δ is the Dirac delta function.

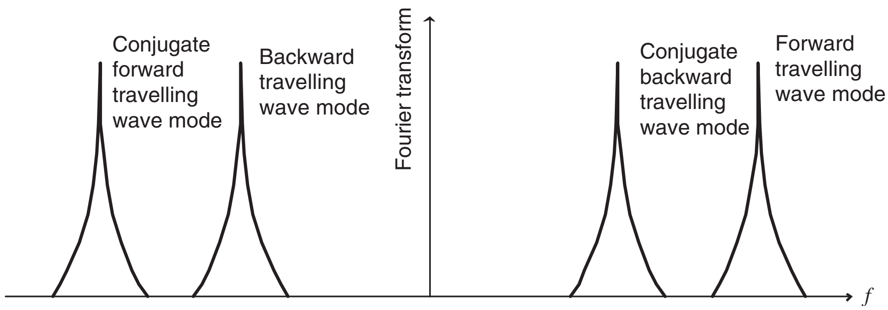

Fig. 7. Example of real frequency analysis.

Eq. (4) shows that when $\sin(n\alpha) = 1$ the effect of the conjugate modal contribution associated with n nodal diameters vanishes. The integral Fourier transform then shows only two peaks: the peak at positive frequencies is related to the forward travelling wave mode while the peak at negative frequencies is related to the backward travelling wave mode. Both tracks in a waterfall plot are right tilted. In other words, separation of the corresponding forward and backward travelling wave modes is achieved when

$$n\alpha = (4k+1)\frac{\pi}{2}, \quad k = 0, 1, 2, \ldots \tag{5}$$

Separation of the corresponding conjugate forward and backward travelling wave modes is achieved when

$$\sin(n\alpha) \quad \text{or} \quad n\alpha = (4k+3)\frac{\pi}{2}, \quad k = 0, 1, 2, \ldots \tag{6}$$

and the corresponding tracks in a waterfall plot are left tilted.

The method was used to analyse the signal obtained with two different phase angles between the sensors: $\alpha = \pi/2$ and $\alpha = \pi/4$. Figs. 8(a) and (b) show the two-sided waterfall diagrams obtained by processing the displacement signals for the two-phase angles, for the entire test period, in the case of an inclined grinding wheel. According to Eqs. (5) and (6), in the considered frequency range, for $\alpha = \pi/2$ the single right-tilted mode tracks correspond to $n = 1$ and the left-tilted ones to $n = 3$, while for $\alpha = \pi/4$ the single right-tilted mode tracks correspond to $n = 2$.

This approach is particularly useful if only data for a single rotational speed are available. Another approach is based on the use of the waterfall spectrum diagram of a displacement signal obtained for different rotational speeds. In this case it is possible to correlate modes and peak tracks by simply considering the dependency of the natural frequency on the rotational speed and in particular the relationship between the track slope and the number of nodal diameters,

$$\begin{cases} \omega_n^+ = \omega_n + n\Omega, \\ \omega_n^- = -(\omega_n - n\Omega), \end{cases} \tag{7}$$

ω_n^+ and ω_n^- being the forward and backward natural frequencies, respectively.

Both approaches were used to gain information about the directivity of the modes and their number of nodal diameters to support the modal analysis carried out on the non-rotating disc.

3.3. Analysis of the sharpening process

In order to better understand the origin of the self-excited vibrations that sometimes arise during the sharpening process, the interval where the grinding wheel is sharpening the edge of the disc and the subsequent interval where the grinding wheel is removed from the disc (sharpening and break periods) were analysed separately. The signals were first filtered in order to lower the low-frequency noise by means of a high-pass filter with a cut-off frequency of 40 Hz. Waterfall plots were obtained from the FFT of the data acquired, at different rotational speeds, by a sensor facing the grinding wheel.

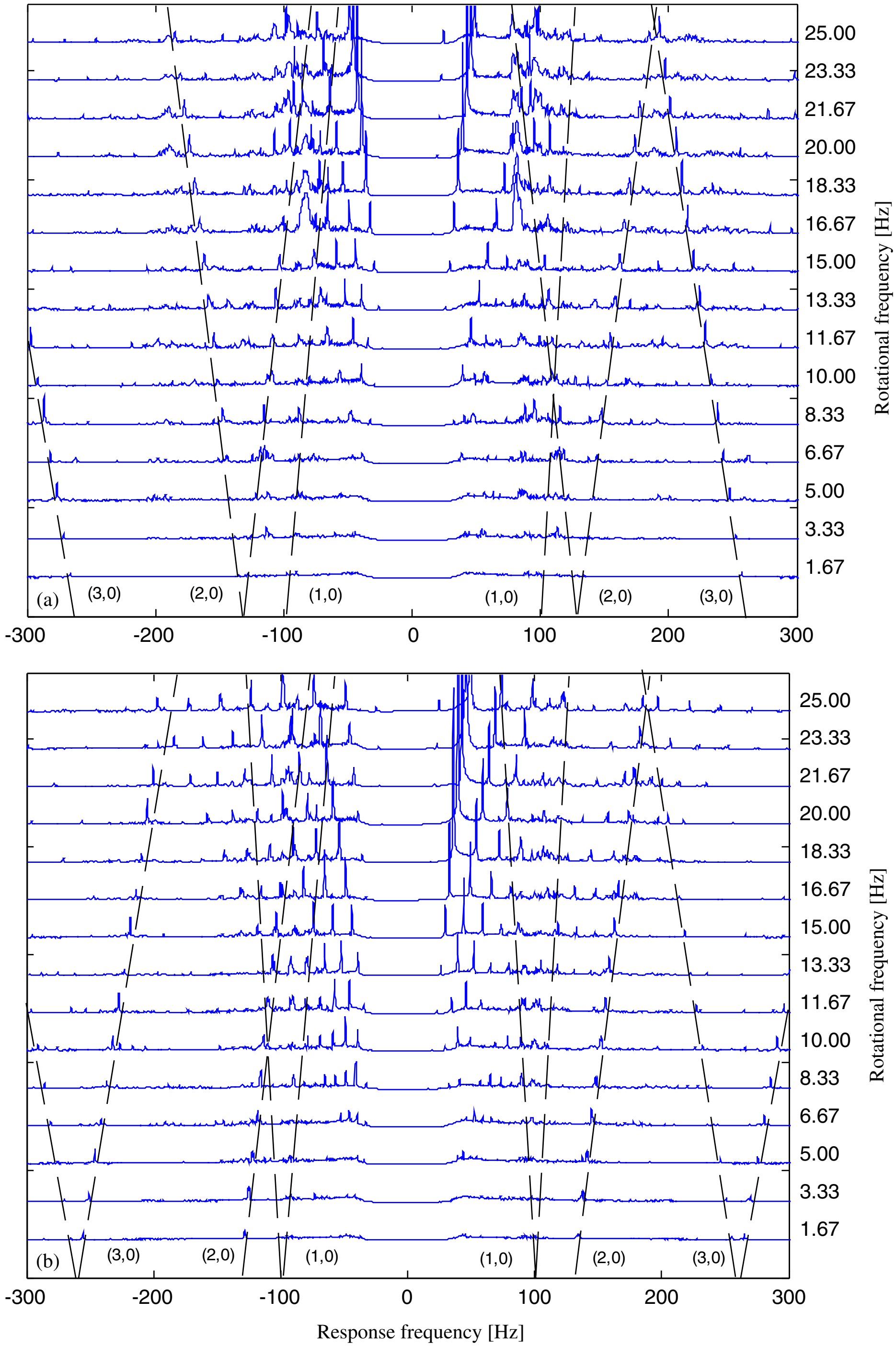

Fig. 8. Waterfall plot processing the displacement signals of two sensors at (a) $\alpha = \pi/2$ and (b) $\alpha = \pi/4$ (intermittent sharpening test and tilted abrasive wheel).

Fig. 9 shows the waterfall plot obtained from the data of the reference test. Fig. 9(a) shows the behaviour of the disc during the second sharpening period of the test sequence while Fig. 9(b) concerns the following break period. The peaks related to the harmonics of the disc rotational speed $1\times$ and $2\times$ are the most pronounced.

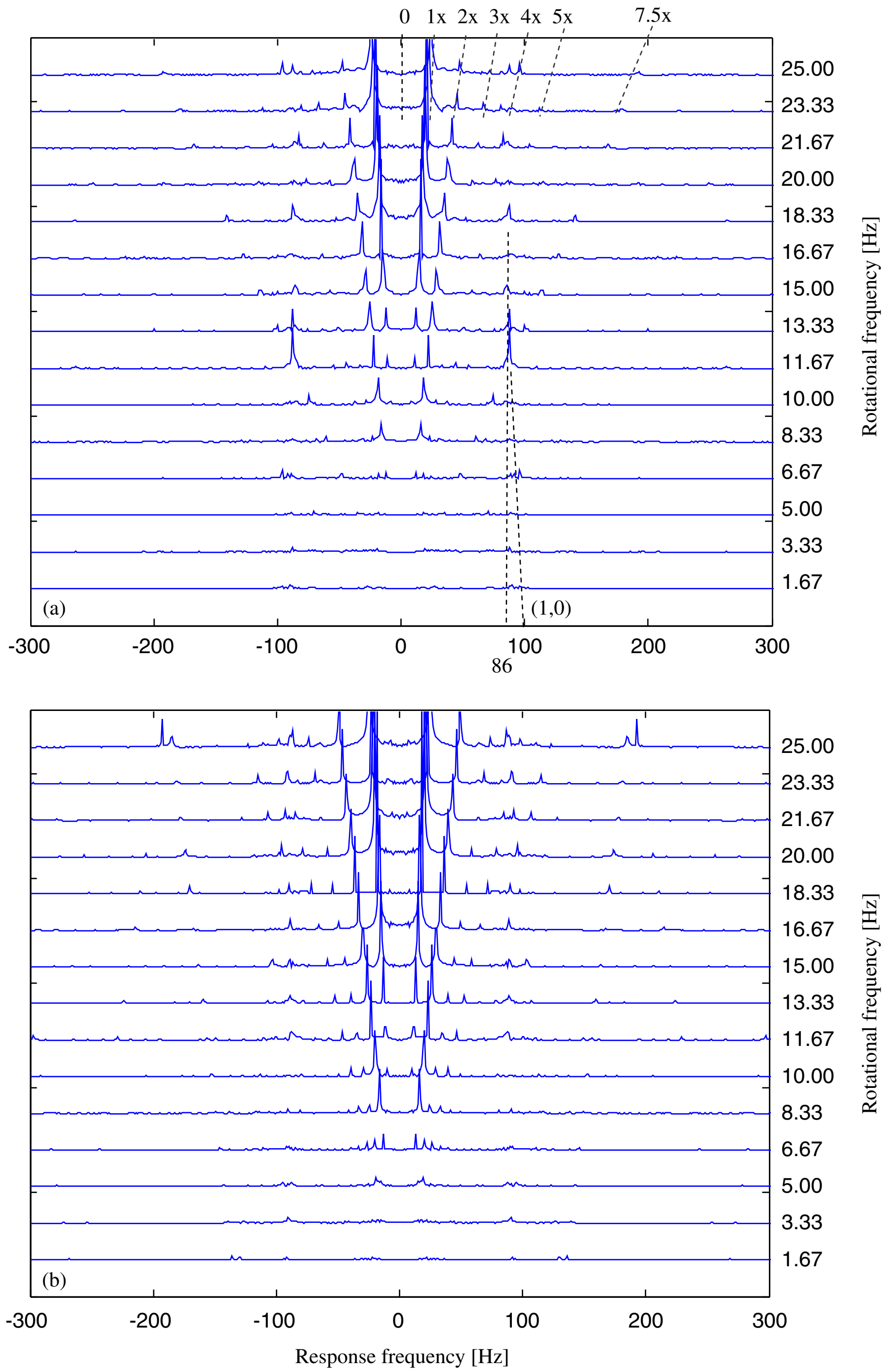

Fig. 9. Waterfall plot of the sharpening phases of the reference test: (a) during and (b) after the sharpening operation.

Such peaks are most probably due to the unavoidable geometric tolerance errors on the disc planarity; in fact, they were noticed also before the first sharpening.

Then a series of peaks aligned around 86 Hz can be noticed. These peaks can be correlated to the 86 Hz vertical mode of the grinding wheel support (see Table 3). Such peaks increase when crossing the harmonics of the disc rotational speed, but the highest peak is recorded at a rotational frequency of 11.67 Hz when the constant frequency track is crossed by both the backward travelling wave (1,0) mode track and the $7.5\times$ harmonic track. The latter corresponds to the rotational frequency of the grinding wheel, 7.5 times the rotational frequency of the disc. So it seems more likely a resonance excited by the grinding wheel rotation rather than a lock-in phenomenon since the tangential friction force is rather low in the idle wheel case. After the sharpening period the 86 Hz peaks disappear as well as the $7.5\times$ harmonic track, as shown in Fig. 9(b). Only the disc speed related frequencies are clearly observed while tracks of forward and backward travelling waves are barely visible.

Further considerations will be deduced from the other experiments discussed in the following section.

3.4. Influence of operating parameters

The test carried out tilting the grinding wheel by 2° in the rotating direction is of particular interest because it is closer to the practical case. In this configuration, the coupling of the vertical vibrations of the grinding wheel with the flexural ones of the disc is possible even with no friction; the tangential force being related to the transverse one simply by the tangent of the grinding wheel tilting angle. However, for a small tilting angle as in this case, the main effect of tilting is the change of contact and friction conditions (Fig. 3). Increasing the tilt angle can only increase the force component perpendicular to the grinding wheel axis and thus the risk of lock-in occurrence.

The test results are shown in Figs. 10(a) and (b). The natural frequency of the grinding wheel sleeve (82 Hz) is slightly lower than in the reference case because of the different configuration and constraints. The harmonic related to the grinding wheel rotational frequency is also lower ($5.5\times$) as expected (cf. par.2.1).

High broad peaks can be seen around 82 Hz in a range of rotational frequencies starting from 16.67 Hz. Again, they can be related to the (1,0) disc and grinding wheel sleeve modes, but this time the $5\times$ and $4\times$ disc harmonics now play a role in exciting vibrations. Higher damping than in the reference case, due to increased sliding friction power loss, broadens the peaks. As for the reference test, after the sharpening period these peaks vanish while the disc speed related frequencies are still present. The tracks of forward and backward travelling waves are here more evident.

As far as the influence of the other parameters is concerned, it was noticed that the 86 Hz peaks and $7.5\times$ harmonic were related to high friction. In fact when the pushing force was reduced thus reducing the friction force (Fig. 11(a)) or when the contact area was sprinkled with water (Fig. 11(b)), there was a significant reduction of the 86 Hz peaks and there was no sign of the $7.5\times$ harmonic. Similar results were obtained when the rotation of the grinding wheel was prevented (Fig. 12) but here the explanation is the absolute absence of the grinding wheel speed related excitation. On the other hand the higher friction power loss due to pure sliding conditions provided high damping and lowered the disc speed related harmonic peaks. A small peak corresponding to the (1,0) disc mode and the 86 Hz grinding wheel sleeve mode, at a disc rotational speed of 13.33 Hz, could suggest the occurrence of lock-in, the peak small amplitude being due to the short transient sharpening period. In any case, the negligible effect of such a phenomenon, in the case of locked wheel where the friction force is considerable, confirms resonance as the main cause of vibration in the case of idle wheel.

A long sharpening time (5 s) increased the disc vibration level. On the contrary, a short sharpening test caused its reduction.

The same trends were observed in the tests on the 1 mm thick disc and for different angular position of the Proximitors®. However, when the vibratory response of the more compliant disc was particularly intense the results were not considered reliable, because of intermittent contact between the disc and the grinding wheel due to bounces.

4. Conclusions

This work, motivated by a paper-cutting problem, can be of interest in other fields wherever the sharpening process involves a circular blade. Reduction of vibrations in the sharpening process is important to obtain a blade edge straight profile and to ensure a precise cut by the blade.

The paper described the design of a test rig for the study of the vibratory behaviour of a rotating disc subjected to a sharpening process. An experimental campaign was carried out and the vibrational

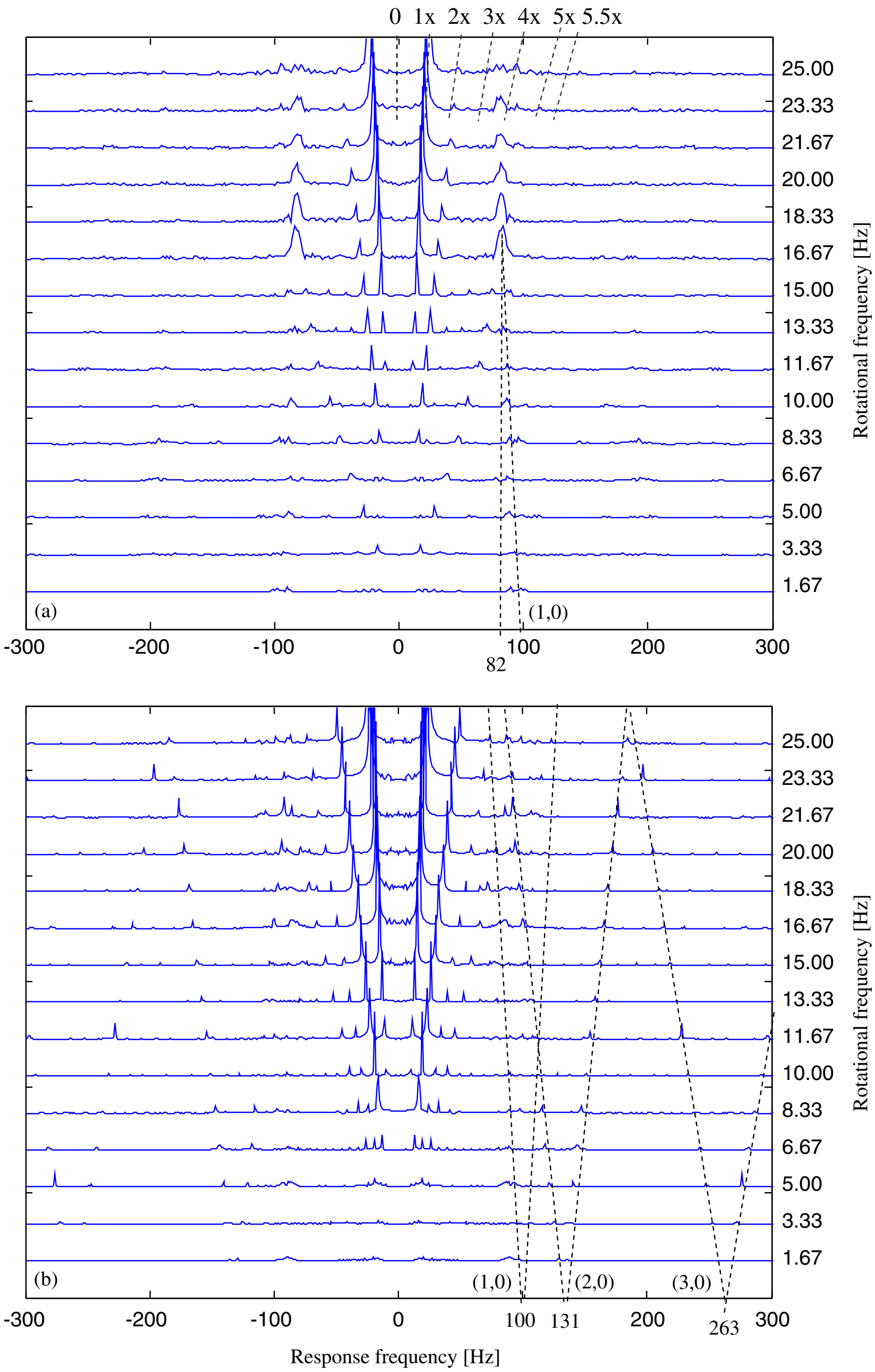

Fig. 10. Waterfall plot of the sharpening phases of the tilted wheel test: (a) during and (b) after the sharpening operation.

behaviour of the rotating disc was characterized pointing out the natural modes and the resonance conditions. The test rig made it possible to carry out a series of tests varying the process parameters such as the grinding contact force, duration and relative position of the two mating elements, the disc rotating speed, the spring stiffness and the friction coefficient, in order to point out the most important variables for the system vibrations.

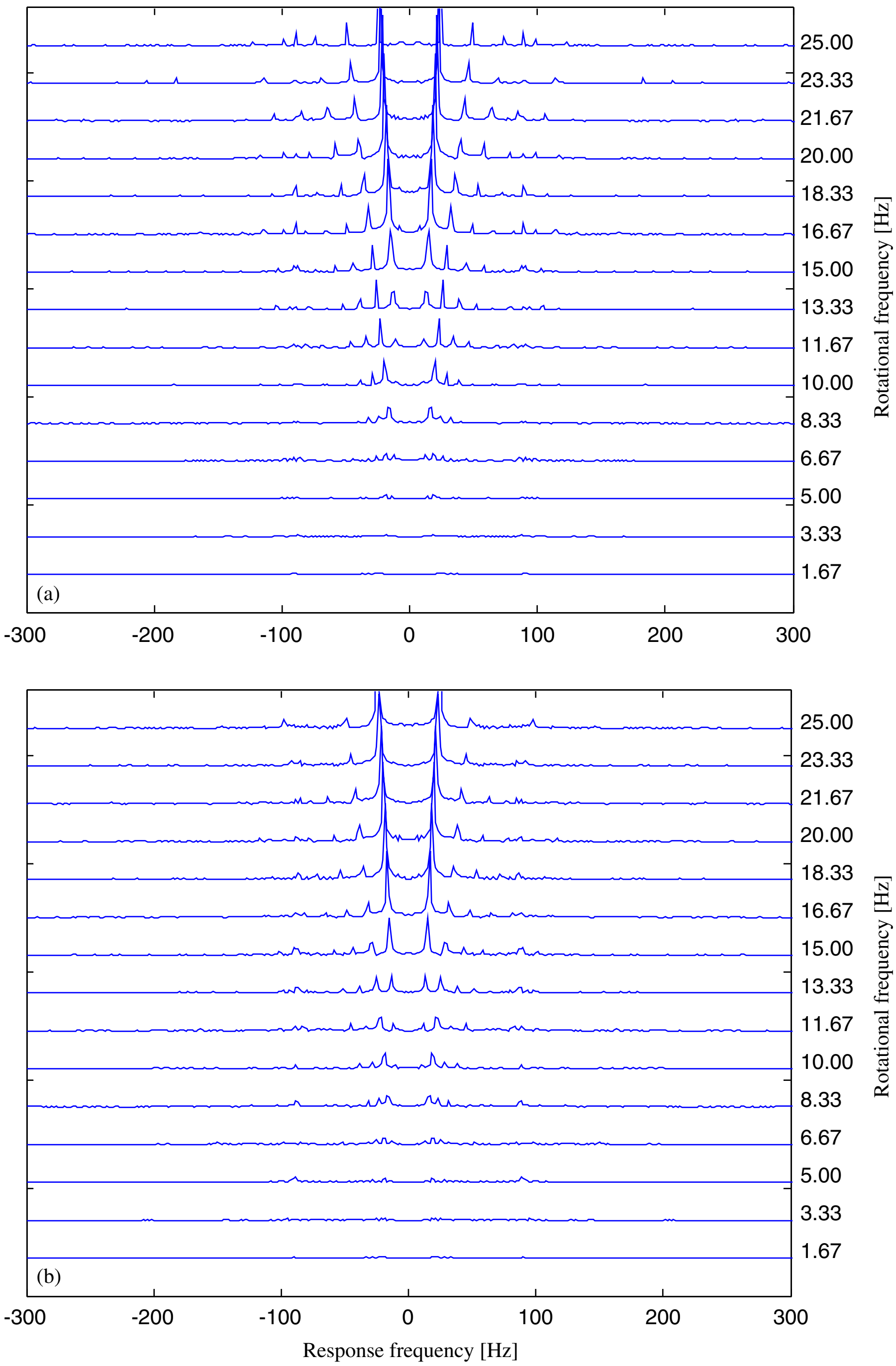

Fig. 11. Waterfall plot of the sharpening interval; test carried out (a) reducing the spring pre-load, (b) reducing the contact friction by water lubrication.

From the analysis of the sharpening process of the reference test we can conclude that the highest vibration level can be ascribed to a resonance phenomenon due to the grinding wheel rotation exciting a grinding wheel support mode and a disc mode coupled by contact friction. A careful analysis of the natural frequencies of the two components, taking into account their operating rotating speeds, can avoid that phenomenon.

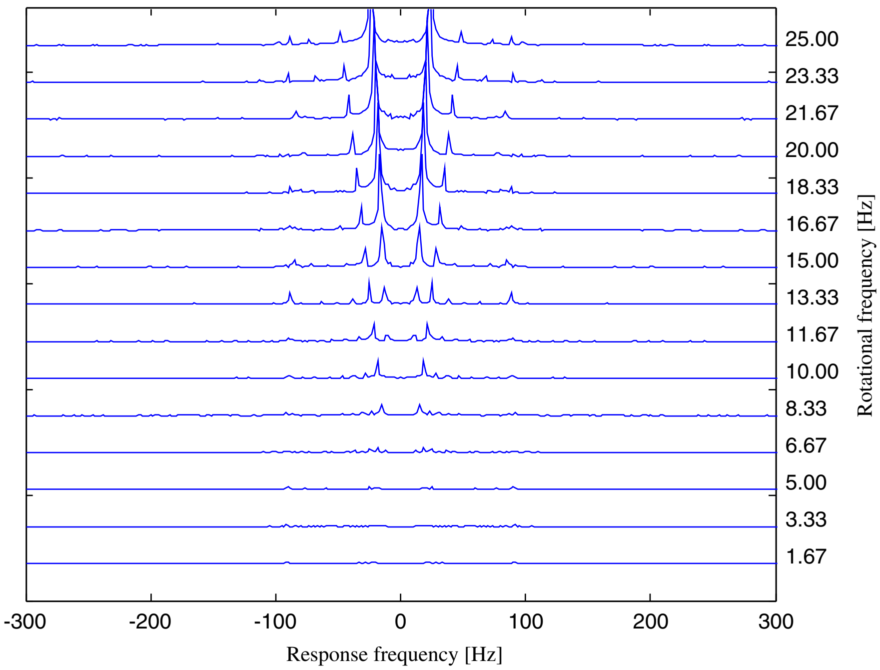

Fig. 12. Waterfall plot of the sharpening interval; test carried out with no rotation of the grinding wheel.

From the analysis of all the results, even though limited to the particular values of the parameters considered, some characteristic trends on the influence of the sharpening parameters on the disc vibrations can be summarised as follows. Tilting the abrasive wheel axis, necessary for the sharpening process, can cause a significant increase in the resonance vibration amplitudes and the broadening of resonance peaks in a range of rotational speeds, due to different contact and friction conditions. It should be kept as low as possible also to avoid lock-in phenomena. The vibration level can be reduced by lowering the spring pre-load, sprinkling the disc with water, locking the rotational displacement of the grinding wheel and reducing the sharpening time. However, such parameters and operating conditions must be carefully considered because friction reduction degrades the abrasive property of the grinding wheel and lengthens the sharpening process and the locking of the grinding wheel increases tool wear and maintenance needs. A solution could be that of a controlled rotation of the grinding wheel.

Finally, no experimental evidence was obtained of eventual lock-in instability phenomena in the case of idle grinding wheel due to the low disc tangential force with respect to the transverse force.

References

[1] B. Bartalucci, G. Lisini, P. Pinotti, Grinding at variable speed, in: S. Tobias, F. Koenigsberger (Eds.), *Advances in Machines Tool Design and Research*, Pergamon Press, Geneva, 1971, pp. 633–652.

[2] S. Huang, W. Chiou, Modeling and vibration analysis of spinning-disk and moving-head assembly in computer storage system, *Transactions of the ASME Journal of Vibration and Acoustics* 119 (1997) 185–191.

[3] I. Shen, Recent vibration issues in computer hard disk drives, *Journal of Magnetism and Magnetic Materials* 209 (2000) 6–9.

[4] J. Mottershead, S. Chan, Brake squeal—an analysis of symmetry and flutter instability, in: R. Ibrahim, A. Soom (Eds.), *Friction-Induced Vibration, Chatter, Squeal, and Chaos*, Vol. ASME DE-49, Elsevier Science Publishers, New York, 1992, pp. 87–97.

[5] R. Ibrahim, Friction-induced vibration, chatter, squeal, and chaos: part II—dynamics and modeling, in: R. Ibrahim, A. Soom (Eds.), *Friction-Induced Vibration, Chatter, Squeal, and Chaos*, Vol. ASME DE-49, Elsevier Science Publishers, New York, 1992, pp. 123–138.

[6] T. Hamabe, I. Yamazaki, K. Yamada, H. Matsui, S. Nakagawa, M. Kawamura, Study of a method for reducing drum brake squeal, *SAE Transactions* 108 (1999) 523–529.

[7] S.A. Tobias, R.N. Arnold, The influence of dynamical imperfection on the vibration of rotating disks, *Proceedings of Mechanical Engineers* 171 (1957) 669–690.

[8] Y. Honda, H. Matsuhisa, S. Sato, Modal response of a disk to a moving concentrated harmonic force, *Journal of Sound and Vibration* 102 (4) (1985) 457–472.

[9] W.D. Iwan, T.L. Moeller, The stability of a spinning elastic disk with a transverse load system, *Journal of Applied Mechanics, Transactions ASME* (1976) 485–490.

[10] C.J. Radcliffe, C.D. Mote Jr., Identification and control of rotating disk vibration, *Journal of Dynamic Systems, Measurement and Control, Transactions ASME* 105 (1) (1983) 39–45.

[11] I. Bucher, P. Schmiechen, D.A. Robb, D.J. Ewins, A laser-based measurement system for measuring the vibration on rotating discs, *Proceedings of the First International Conference on Vibration Measurement by Laser Techniques*, Ancona, Italy, October, 1994.

[12] C.W. Lee, M.E. Kim, Separation and identification of travelling wave modes in rotating disk via directional spectral analysis, *Journal of Sound and Vibration* 187 (1995) 851–864.

[13] D. Lee, A.M. Waas, Stability analysis of a rotating multi-layer annular plate with a stationary frictional follower load, *International Journal of Mechanical Science* 39 (10) (1997) 1117–1138.

[14] A. Tuchinda, N.P. Hoffmann, D.J. Ewins, W. Keiper, Mode lock-in characteristics and instability study of the pin-on-disc system, *Proceedings of the nineteenth International Modal Analysis Conference—IMAC*, Vol. 1, 2001, pp. 71–77.

[15] H. Ouyang, J. Mottershead, M. Cartmell, M. Friswell, Friction-induced parametric resonance in disks: effect of a negative friction-velocity relationship, *Journal of Sound and Vibration* 209 (2) (1998) 251–264.

[16] C. Carmignani, P. Forte, E. Rustighi, Theoretical and experimental investigation on the dynamic behaviour of disc blades during sharpening, *Proceedings of IFToMM Sixth International Conference on Rotor Dynamics*, Vol. 2, Sydney, Australia, 2002, pp. 936–943.